ELSEVIER

Numerical study on the instability of premixed plane flames in the three-dimensional field

Satoshi Kadowaki
Department of Mechanical Engineering, Nagoya Institute of Technology, Nagoya, Japan

The instability of premixed plane flames in the three-dimensional (3-D) field is investigated by means of the numerical simulation. We show numerically that infinitesimal disturbances superimposed on the flames grow exponentially with time, as predicted in the linear analysis, and obtain the growth rates of disturbances depending on the absolute values of the wave-number vectors. The growth rates of the 3-D flames are consistent with those of the two-dimensional (2-D) flames. The hydrodynamic effect has a destabilizing influence on the instability of flames, and the diffusive-thermal effect has a destabilizing/stabilizing influence for $Le < 1/Le > 1$. Moreover, we produce the hexagonal cellular structure of the flame front not only for $Le < 1$ but also for $Le > 1$, where the spacing between cells in flames for $Le < 1$ is small compared to that for $Le > 1$. The spacing of the 3-D flames is $2/\sqrt{3}$ times as long as the cell size of the 2-D flames.

Keywords: numerical simulation; flame instability; cellular flame

Introduction

It is well known that three fundamental effects are responsible for the inherent instability of premixed flames: the hydrodynamic effects; the diffusive-thermal effect; and the body-force effect (Williams 1985). The hydrodynamic and diffusive-thermal effects are especially important factors on the flame instability.

The hydrodynamic effect originates in thermal expansion through the flame front. The classical analysis on the stability of slow burning flames in which the flame front was treated as a discontinuous surface showed that the flames are absolutely unstable (Darrieus 1938; Landau 1944). Subsequently, the hydrodynamic flame stability taking account of a preheat zone with finite thickness was investigated by several researchers (Pelce and Clavin 1982; Matalon and Matkowsky 1982; Frankel and Sivashinsky 1982; Kadowaki and Tsuge 1985). The dispersion relation asymptotic to the classical solution for sufficiently small wave numbers was acquired, and the marginal wave number separating the stable region was determined. The results indicated that the flames are stable for disturbances with wave numbers larger than the marginal wave number; namely, the flames shorter than the marginal wavelength, corresponding to the marginal wave number, are stable. Recently, the instability of a deflagration wave propagating with considerably fast velocity was analyzed, and it was shown that the growth rate is larger than that for slow burning flames (Kadowaki 1995a).

The diffusive-thermal effect is caused by imbalance between the diffusivity of reactant and the thermal diffusivity. It was observed in the experiment that cellular flames are strongly affected by the diffusive-thermal effect (Markstein 1951). The diffusive-thermal instability appears when the Lewis number of the deficient reactant is smaller than the critical value (Barenblatt et al. 1962). The diffusive-thermal theory in which the density of gases is set equal to a constant led to the conclusion that the flame front is unstable in small wave-number region for sufficiently small Lewis numbers (Sivashinsky 1977; Joulin and Mitani 1981). In the theory, the hydrodynamic effect is neglected, and, hence, the diffusive-thermal model is valid only for small enough heat release.

The numerical simulation is a very useful method to study the instability of flames. For example, stable/unstable motions of rich/lean premixed hydrogen–oxygen flames using a detailed chemical reaction model was calculated (Patnaik et al. 1988), the reduced evolution equations for the flame front were numerically solved (Michelson and Sivashinsky 1982; Thual et al. 1985; Denet and Haldenwang 1992, 1995; Denet 1993), and the hydrodynamic and diffusive-thermal effects on the instability of freely expanding cylindrical flames were researched (Kadowaki 1995b).

In the linear analysis, it is necessary to assume that the amplitude of disturbance on the flames is infinitesimal. In the numerical simulation, on the other hand, such an assumption is needless. Therefore, we can deal with the disturbed flame where the amplitude is considerably large and can study the mechanism of the cellular flame formation.

We have already investigated the instability of premixed plane flames and the formation of cellular flames in the two-dimensional (2-D) field by means of the numerical simulation. We obtained the dispersion relation, which is tallied with the result of the linear analysis on the hydrodynamic flame instability, and elucidated that the cell size of the 2-D flames is equivalent to the wavelength of the disturbance with the maximum growth rate

Address reprint requests to Satoshi Kadowaki, Department of Mechanical Engineering, Nagoya Institute of Technology, Gokiso-cho, Showa-ku, Nagoya 466, Japan.

Received 8 March 1996; accepted 20 May 1996

Int. J. Heat and Fluid Flow 17: 557–566, 1996

655 Avenue of the Americas, New York, NY 10010

0142-727X/96/$15.00
PII S0142-727X(96)00066-X

(Kadowaki 1994). Under most experimental conditions, however, the three-dimensional (3-D) flames are usually formed. The 2-D flames are seldom observed, because they require a special experimental setup. Therefore, it is very important to investigate the flame instability in the 3-D field. Furthermore, it was reported that the mean spacing between cells of the 3-D flames is always large compared to the cell size of the 2-D flames (Strehlow 1968). To solve this problem, we have to study the formation of cellular flames in the 3-D field.

In this study, we calculate the evolution of the disturbed flame in the 3-D field and obtain the dispersion relation to compare with the result in the 2-D field and to examine the hydrodynamic and diffusive-thermal effects. Moreover, we study the mechanism of the cellular flame formation and show the relation between the cell sizes of the 2- and 3-D flames.

Governing equations

We consider single-reactant flames, where the abundant component is excess, and the reaction is controlled only by the deficient component. We take the direction of the main flow as the x-direction and the surface of the flame front as the yz-surface. The assumptions used in this study are as follows.

(1) Only two species, unburned and burned gases, are present. Both gases are ideal and have the same molecular weights and the same Lewis numbers.

(2) The chemical reaction is an exothermic irreversible one-step reaction, and the reaction rate has the Arrhenius form.

(3) All transport coefficients are constant throughout the whole region.

(4) The radiation, the bulk viscosity, the Soret effects, the Dufour effects, and the pressure gradient diffusion are negligible, and the viscous term in the energy equation is disregarded.

We start from the conservation equations of the 3-D reactive flows including compressibility, viscosity, heat conduction, and molecular diffusion, and the equation of state. The flow variables in the equations are nondimensionalized by the characteristic length (80 times as long as the preheat zone thickness), the characteristic velocity (the isothermal sound velocity of the unburned gas), and the density of the unburned gas. The governing equations are written in conservation form as

$$\frac{\partial \mathbf{U}}{\partial t}+\frac{\partial \mathbf{F}}{\partial x}+\frac{\partial \mathbf{G}}{\partial y}+\frac{\partial \mathbf{H}}{\partial z}=\mathbf{S} \tag{1}$$

where **U**, **F**, **G**, **H**, and **S** are vectors given by

$$\mathbf{U}=\begin{pmatrix}\rho\\ \rho u\\ \rho v\\ \rho w\\ e\\ \rho Y\end{pmatrix}$$

$$\mathbf{F}=\begin{pmatrix}\rho u\\ \rho u^2+p-\dfrac{\mathrm{Pr}}{\mathrm{Pe}}\left(\dfrac{4}{3}\dfrac{\partial u}{\partial x}-\dfrac{2}{3}\dfrac{\partial v}{\partial y}-\dfrac{2}{3}\dfrac{\partial w}{\partial z}\right)\\ \rho uv-\dfrac{\mathrm{Pr}}{\mathrm{Pe}}\left(\dfrac{\partial v}{\partial x}+\dfrac{\partial u}{\partial y}\right)\\ \rho uw-\dfrac{\mathrm{Pr}}{\mathrm{Pe}}\left(\dfrac{\partial w}{\partial x}+\dfrac{\partial u}{\partial z}\right)\\ (e+p)u-\dfrac{1}{\mathrm{Pe}}\dfrac{\gamma}{\gamma-1}\dfrac{\partial T}{\partial x}\\ \rho Yu-\dfrac{1}{\mathrm{Pe\,Le}}\dfrac{\partial Y}{\partial x}\end{pmatrix}$$

$$\mathbf{G}=\begin{pmatrix}\rho v\\ \rho uv-\dfrac{\mathrm{Pr}}{\mathrm{Pe}}\left(\dfrac{\partial v}{\partial x}+\dfrac{\partial u}{\partial y}\right)\\ \rho v^2+p-\dfrac{\mathrm{Pr}}{\mathrm{Pe}}\left(\dfrac{4}{3}\dfrac{\partial v}{\partial y}-\dfrac{2}{3}\dfrac{\partial u}{\partial x}-\dfrac{2}{3}\dfrac{\partial w}{\partial z}\right)\\ \rho vw-\dfrac{\mathrm{Pr}}{\mathrm{Pe}}\left(\dfrac{\partial w}{\partial y}+\dfrac{\partial v}{\partial z}\right)\\ (e+p)v-\dfrac{1}{\mathrm{Pe}}\dfrac{\gamma}{\gamma-1}\dfrac{\partial T}{\partial y}\\ \rho Yv-\dfrac{1}{\mathrm{Pe\,Le}}\dfrac{\partial Y}{\partial y}\end{pmatrix}$$

Notation

A	amplitude
A_0	initial amplitude
B	frequency factor
E	activation energy
e	stored energy
k	absolute value of wave-number vector
k_p	peculiar wave number
k_y, k_z	y, z components of wave-number vector
Le	Lewis number
N	positive integer
Pe	Peclet number
Pr	Prandtl number
p	pressure
Q	heating value
T	temperature
t	time
u, v, w	x, y, z components of velocity
x, y, z	Cartesian coordinates
Y	mass fraction of unburned gas

Greek

γ	ratio of specific heats
δ	preheat zone thickness
λ_y, λ_z	wavelengths in y, z directions
λ_2	cell size of two-dimensional flames
λ_3	spacing between cells of three-dimensional flames
ρ	density
ω	growth ratio

$$\mathbf{H} = \begin{pmatrix} \rho w \\ \rho uw - \dfrac{\mathrm{Pr}}{\mathrm{Pe}}\left(\dfrac{\partial w}{\partial x} + \dfrac{\partial u}{\partial z}\right) \\ \rho vw - \dfrac{\mathrm{Pr}}{\mathrm{Pe}}\left(\dfrac{\partial w}{\partial y} + \dfrac{\partial v}{\partial z}\right) \\ \rho w^2 + p - \dfrac{\mathrm{Pr}}{\mathrm{Pe}}\left(\dfrac{4}{3}\dfrac{\partial w}{\partial z} - \dfrac{2}{3}\dfrac{\partial u}{\partial x} - \dfrac{2}{3}\dfrac{\partial v}{\partial y}\right) \\ (e+p)w - \dfrac{1}{\mathrm{Pe}}\dfrac{\gamma}{\gamma-1}\dfrac{\partial T}{\partial z} \\ \rho Yw - \dfrac{1}{\mathrm{Pe\,Le}}\dfrac{\partial Y}{\partial z} \end{pmatrix}$$

$$\mathbf{S} = \begin{pmatrix} 0 \\ 0 \\ 0 \\ 0 \\ QB\rho Y \exp(-E/T) \\ -B\rho Y \exp(-E/T) \end{pmatrix}.$$

The equation of state is

$$p = \rho T \tag{2}$$

Numerical procedures

The physical parameters are given to simulate a gas mixture of which the burning velocity is 0.83 m/s, and the adiabatic flame temperature is 2086 K at atmospheric pressure and room temperature. Nondimensional burning velocity and adiabatic flame temperature are 2.5×10^{-3} and 7.0, respectively. Nondimensional parameters used in the calculation are $\mathrm{Pe} = 3.2 \times 10^4$, $\mathrm{Pr} = 1.0$, $\gamma = 1.4$, $Q = 21$, and $E = 70$. For examining the diffusive-thermal effect on the flame instability, $\mathrm{Le} = 0.5, 0.8, 1.0, 1.2$ are taken. The frequency factor is determined by the condition that the burning velocity of the 1-D flame is equal to the set burning velocity ($= 2.5 \times 10^{-3}$). The frequency factors for $\mathrm{Le} = 0.5, 0.8, 1.0, 1.2$ are 2.2×10^6, 1.4×10^6, 1.2×10^6, and 1.0×10^6, respectively.

Initial conditions for the 3-D flames are provided with the solution of the 1-D flame. On the flame, we superimpose a small sinusoidal disturbance periodic in the y- and z-directions. The displacement of the flame front in the x-direction due to the disturbance is given by

$$A_0 \sin(2\pi y/\lambda_y)\sin(2\pi z/\lambda_z) \tag{3}$$

In the 2-D flames, the displacement is $A_0 \sin(2\pi y/\lambda_y)$.

Boundary conditions are as follows. In the x-direction, except for the velocity of inlet flow, free flow conditions are employed upstream and downstream, and we appropriate one-sided difference approximations with second-order accurate. The flow velocity upstream is set to the burning velocity, to the end that the flame position barely moves. In the y- and z-direction, spatially periodic conditions are used.

The explicit MacCormack scheme, which has second-order accuracy in both time and space, is adopted for the calculation. A computational domain is the characteristic length in the x-direction and one wavelength of disturbance in the y- and z-directions, which is resolved by a $161 \times 33 \times 33$ variably spaced grid for the dispersion relation and by a $201 \times 31 \times 53$ grid for the cellular flame. These grids are fine to prevent numerical errors from contaminating the solutions. The time increment is 5×10^{-4}. For one time step, required CPU times are 0.08-s and 0.15-s for the $161 \times 33 \times 33$ and $201 \times 31 \times 53$ grids, respectively, on a FUJITSU VP2600/10 supercomputer. Each computation time ranges between 1 and 7 h.

The disturbance superimposed on the flame will grow with time. The growth rate of disturbance is defined as

$$\omega = \frac{\mathrm{d}}{\mathrm{d}t} \ln(A/A_0) \tag{4}$$

Results and discussion

Dispersion relation

In this section, to investigate the flame instability, we set the initial amplitude of disturbance to a sufficiently small value ($A_0 = 1 \times 10^{-3}$). The structures of the disturbed flame front at each time (a, $t = 0$; b, $t = 10$; c, $t = 20$) for $\mathrm{Le} = 0.5$, $\lambda_y = \lambda_z = 0.64$ are illustrated in Figure 1. The position of the flame front is defined as the position where $T = 5$. The unburned gas flows in from the bottom, and the burned gas flows out to the top. The amplitude of disturbance becomes greater with time, and then the disturbance on the flame belongs to the parameter group promoting the instability. The amplitude growth rate of disturbance is shown in Figure 2. The ordinate in this figure is the natural logarithm of the ratio of the amplitude to the initial amplitude. From the figure, we know that the disturbance grows exponentially with time ($A \sim e^{\omega t}$), and the growth rate is 7.58×10^{-2}. The linear analysis on the flame instability predicts that infinitesimal disturbances will grow exponentially with time. The result of the calculation is consistent with the prediction of the linear analysis. The behavior of the disturbance, growing exponentially with time, is numerically reproduced only when the amplitude is sufficiently small. When the disturbance grows to some degree, the growth rate is gradually lowered and finally runs down to zero.

To obtain the dispersion relation in the 3-D field, we introduce the absolute value of the wave-number vector of the disturbance

$$k = (k_y^2 + k_z^2)^{1/2} \tag{5}$$

where k_y and k_z are defined as $k_y = 2\pi/\lambda_y$; $k_z = 2\pi/\lambda_z$. In the above case ($\lambda_y = \lambda_z = 0.64$), the absolute value of the wave-number vector is 14. By changing the wavelength of disturbance superimposed on the plane flame ($\lambda_y = \lambda_z = 0.64 \sim 0.128$, $k = 14 \sim 69$), we obtain the growth rates depending on the absolute values of the wave-number vectors. The growth rates are plotted in Figure 3. The dispersion relation in the 3-D field is consistent with that in the 2-D field. In addition, we acquire the same result when $\lambda_y \neq \lambda_z$. On the instability of premixed plane flames, therefore, we can similarly treat both fields. The growth rate is positive for small wave numbers, and there is the marginal wave number ($= 77$). The flames are stable/unstable for disturbances with wave numbers larger/smaller than the marginal wave number. In other words, the flames are stable/unstable for disturbances with wavelengths shorter/longer than the marginal wavelength. Thus, the flames shorter/longer than the marginal wavelength are stable/unstable.

We take $\mathrm{Le} = 0.8, 1.0, 1.2$ for examining the diffusive-thermal effect. The hydrodynamic effect is shown in $\mathrm{Le} = 1.0$ case. The growth rates depending on the absolute values of the wave-number vectors are plotted in Figure 4. The dispersion relations in the 2- and 3-D fields consist with each other. The calculated dispersion relations are similar to the results of the linear analysis on the hydrodynamic flame instability. The growth rates

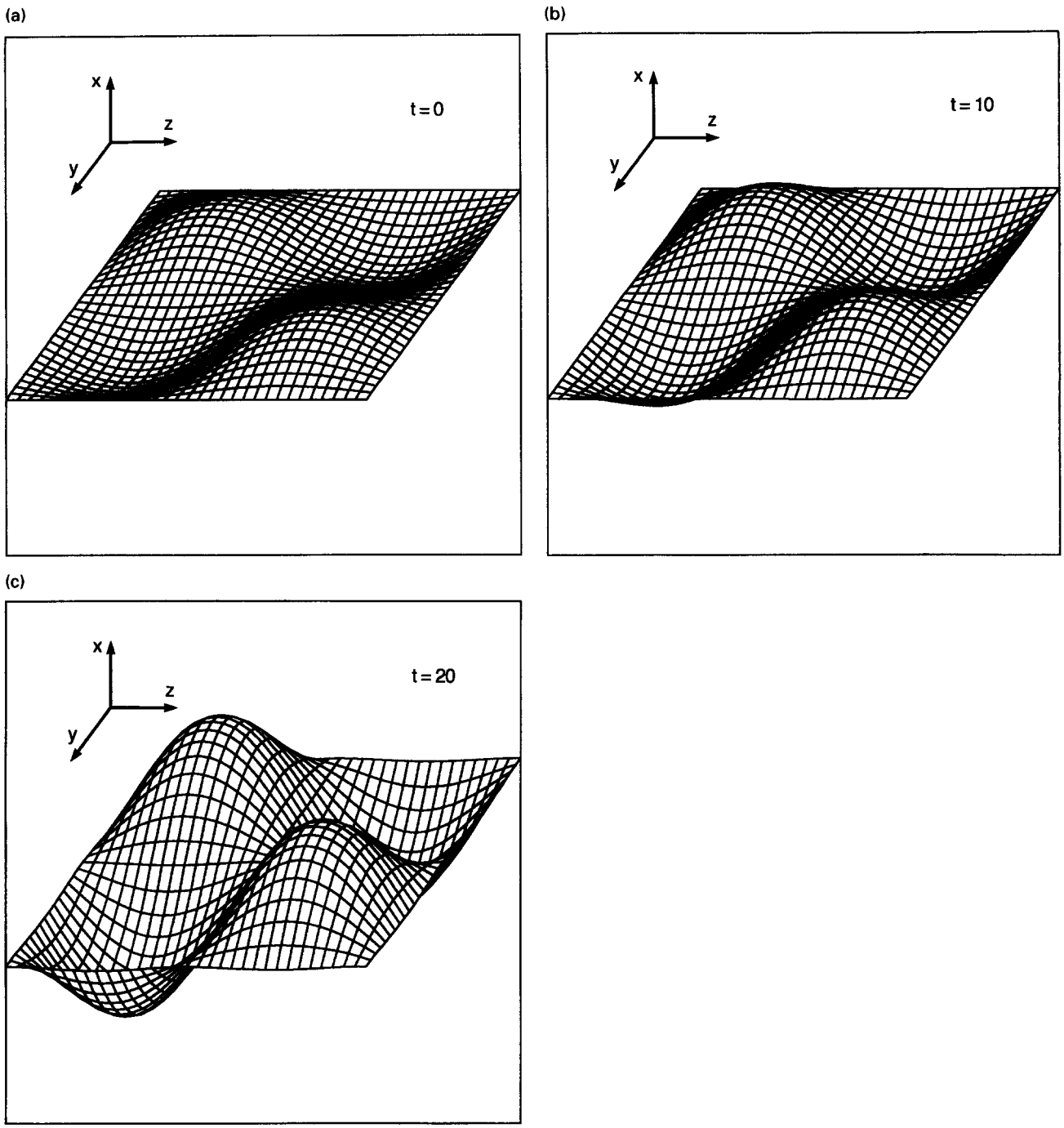

Figure 1 Evolution of the disturbed flame front for Le=0.5, $\lambda_y=\lambda_z=0.64$, $A_0=1\times10^{-3}$ (t=0, 10, 20)

increase, and the unstable region becomes wider for Le = 0.8; whereas, the former decrease and the latter becomes narrower for Le = 1.2. The marginal wave numbers for Le = 0.8, 1.0, 1.2 are 49, 29, and 18, respectively. It means that the diffusive-thermal effect has a destabilizing influence for Le < 1 and has another one for Le > 1. The mechanism of the diffusive-thermal instability is as follows. A convex flame front toward the unburned gas focuses the reactant ahead of the flame (raising the local temperature) and defocuses the heat (reducing the local temperature). On the other hand, a concave flame front defocuses the reactant and focuses the heat. When the diffusivity of reactant is greater than the thermal diffusivity (Le < 1), the local temperature is raised/reduced and the local flame speed increases/decreases at the protruding/receding segment. Therefore, flames for Le < 1 become unstable owing to the diffusive-thermal effect. Similar argument shows that the diffusive-thermal effect has a stabilizing influence for Le > 1 (Law 1988).

Cellular flame

In the previous section, we dealt with sufficiently small disturbances. To study the formation of hexagonal cellular flames, in this section, we treat disturbances with considerably large ampli-

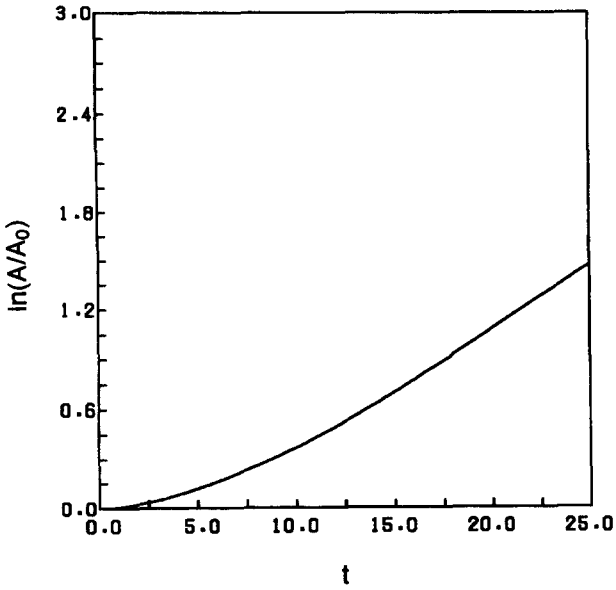

Figure 2 Amplitude growth rate of disturbance for Le=0.5, $\lambda_y=\lambda_z=0.64$, $A_0=1\times10^{-3}$

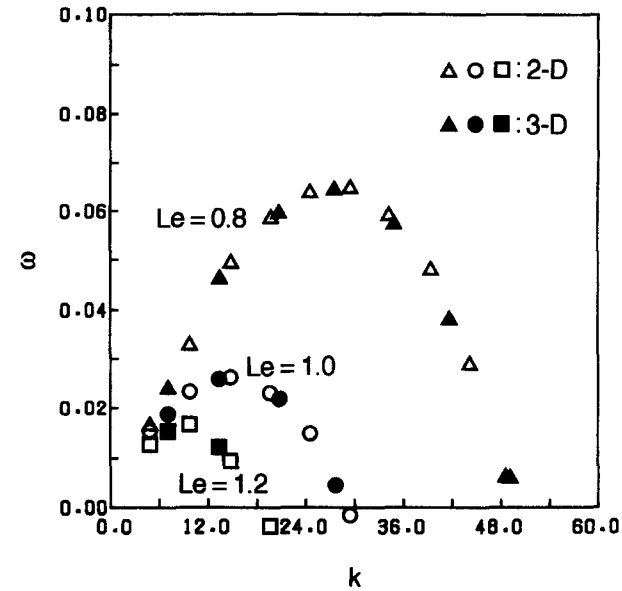

Figure 4 Dispersion relations in both fields for Le=0.8, 10, 1.2; the wave numbers in the 2-D and 3-D fields are 4.9 ~ 49 and 6.9 ~ 49, respectively

tudes. It is impossible to solve this problem by means of the linear analysis, because it is effective in sufficiently small amplitudes.

From the experiment, we know that well-regulated hexagonal cells are formed in sufficiently broad flame surface (Searby and Quinard 1990). Thus, the following relation is required:

$$\lambda_z=\sqrt{3}\,\lambda_y \tag{6}$$

Substituting this relation into Equation 5, we have

$$\lambda_y=\frac{2}{\sqrt{3}}\frac{2\pi}{k} \tag{7}$$

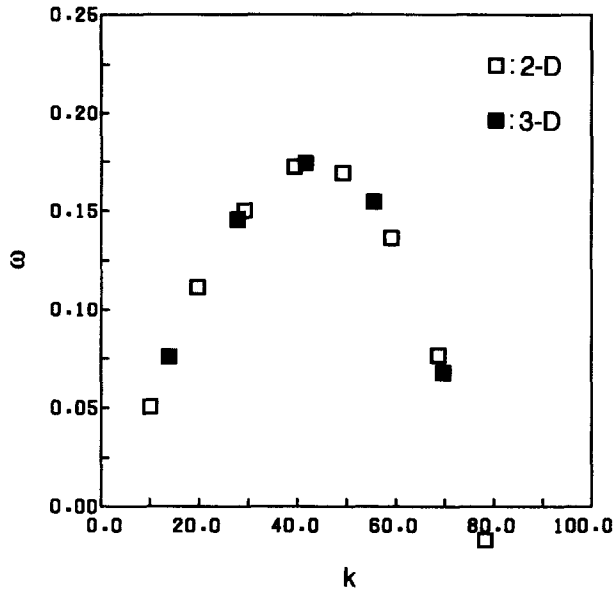

Figure 3 Dispersion relations in both fields for Le=0.5; the wave numbers in the 2-D and 3-D fields are 9.8 ~ 79 and 14 ~ 69, respectively

We find the peculiar wave number (the wave number of the disturbance with the maximum growth rate) from the dispersion relation and determine the peculiar wavelength corresponding to k_p.

We choose Le = 0.5, where the hydrodynamic and diffusive-thermal instabilities affect the cellular flame formation. From Figure 3, we find that $k_p=43.7$, and then $\lambda_y=0.166$, $\lambda_z=0.288$ ($=\sqrt{3}\,\lambda_y$). The disturbance with the peculiar wavelength is superimposed on the plane flame to produce numerically the hexagonal cellular structure of the front. The evolution of the disturbed flame front ($t=0$, 12, 15) is illustrated in Figure 5. At the beginning (up to $t=10$), the disturbance grows exponentially with time. Thereafter, the growth rate is gradually lowered, and the structure of the flame front changes from a sinusoidal shape to a cellular one. The harmonic wave in the z-direction appears at $t=12$. The solution of the hexagonal membrane has this wave (Christopherson 1940). At $t=15$, the hexagonal cellular structure is produced. The amplitude is 0.070. It is obvious from Figure 6 that the spacing between hexagonal cells is equal to λ_y. In other words, λ_3 is equal to 13.3δ, because δ is 0.0125.

We study the cellular flame formation due only to the hydrodynamic instability. In the flame for Le = 1.0, the disturbance is evolved, and the hexagonal cells are revealed. The distribution of the hexagonal cells is illustrated in Figure 7. The amplitude is 0.160, and λ_3 is 0.494 (= 39.5δ). In addition, the cellular flames are formed also for Le = 1.2 (Figure 8), although the diffusive-thermal effect has a stabilizing influence. The amplitude is 0.180, and λ_3 is 0.666 (= 53.3δ). These results show that the cellular flames can be formed owing only to the hydrodynamic instability. The spacing and the amplitude become larger as the Lewis number increases from 0.5 to 1.2. It was reported that the cells appear not only in lean hydrogen flames but also in rich, and the spacing between cells is lengthened as the equivalence ratio increases (Bregeon et al. 1978; Mitani and Williams 1980). Lean/rich hydrogen flames are correspondent to flames for Le < 1/Le > 1, because the deficient component is hydrogen/oxygen, and the Lewis number is smaller/larger than unity. Thus, the obtained results in the calculation are in qualitative agreement with the experiments.

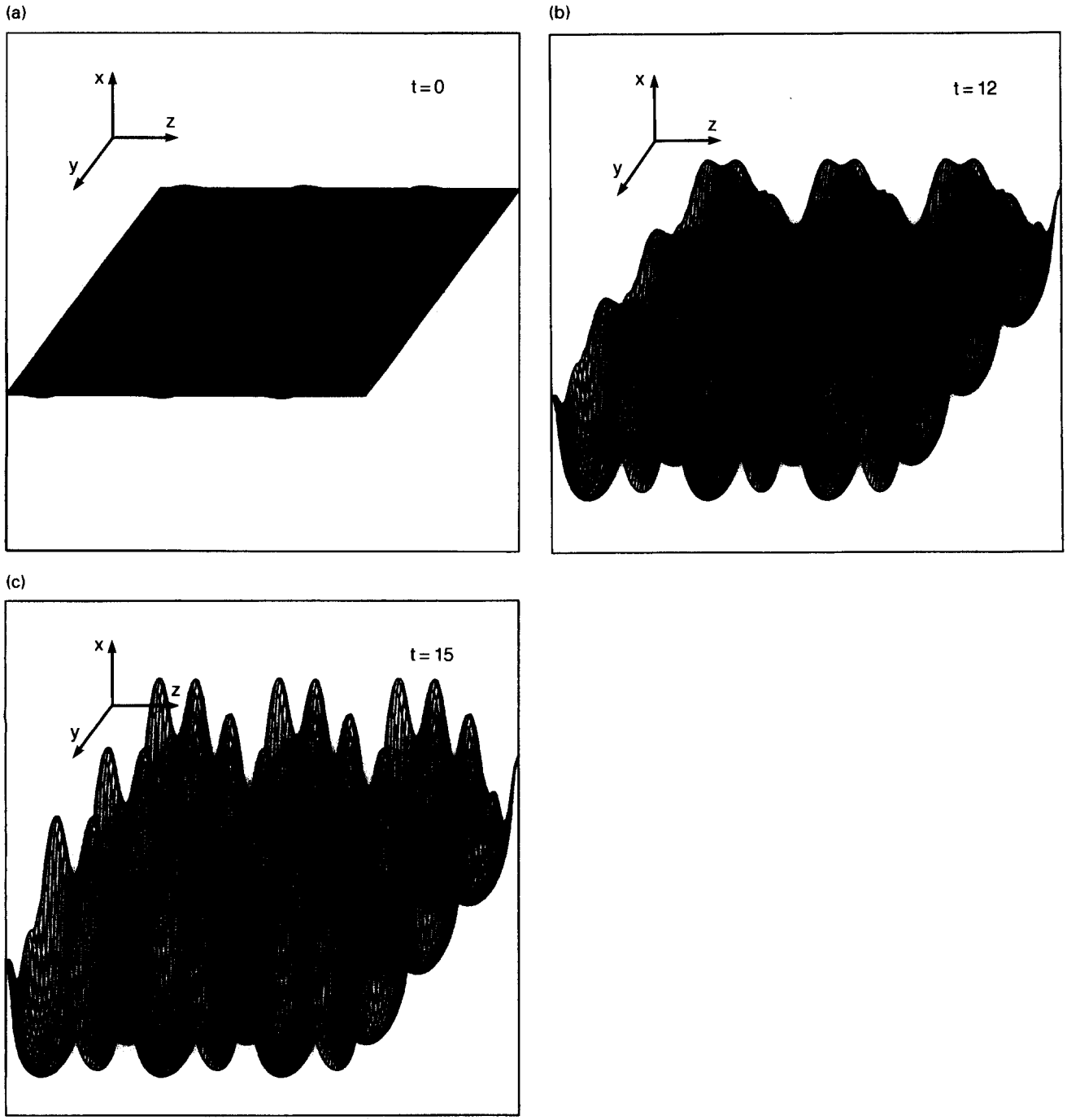

Figure 5 Evolution of the disturbed flame front for Le=0.5, λ_y=0.166, λ_z=0.288, A_0=0.01 (t=0, 12, 15); schematic domain is $3\lambda_y \times 3\lambda_z$

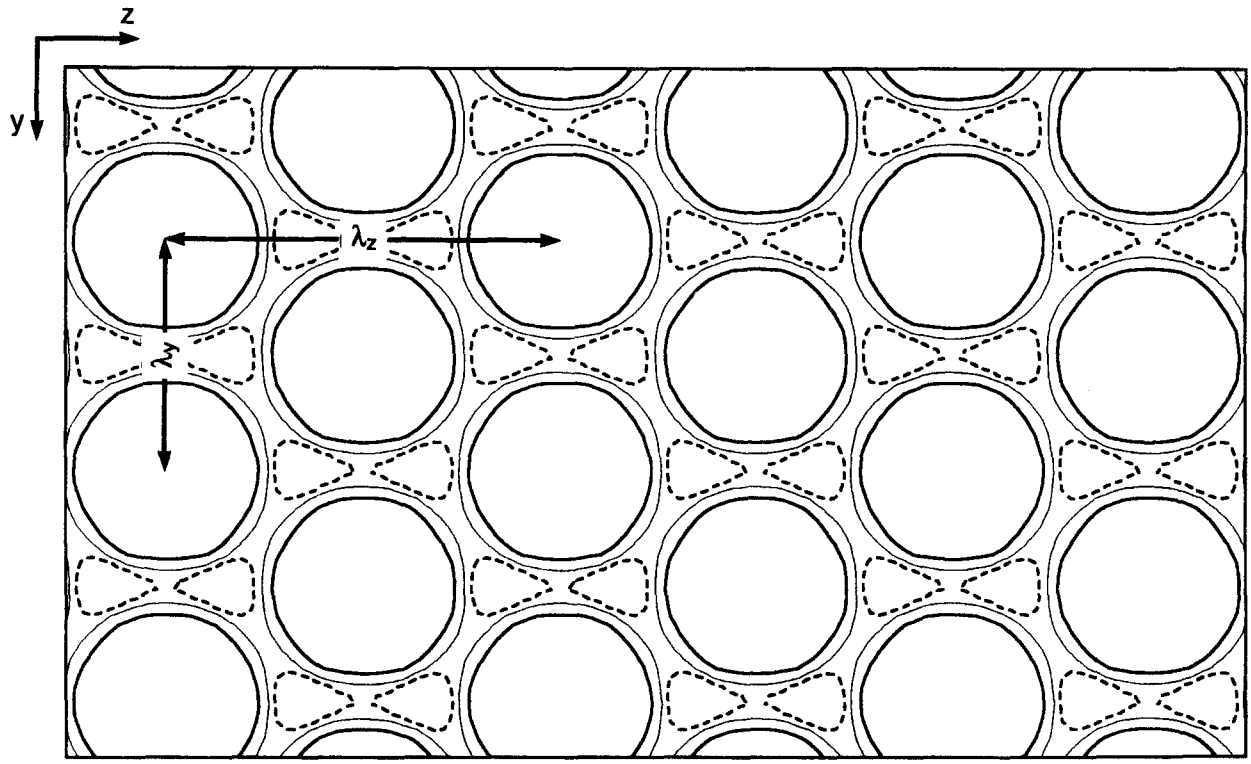

Figure 6 Distribution of the hexagonal cells for Le=0.5, λ_y=0.166, λ_z=0.288, A_0=0.01 (t=15); schematic domain is $3\lambda_y \times 3\lambda_z$; the amplitude is 0.070; solid, hair, and broken lines denote contours of the flame front at x=0.466, 0.501, 0.536, respectively

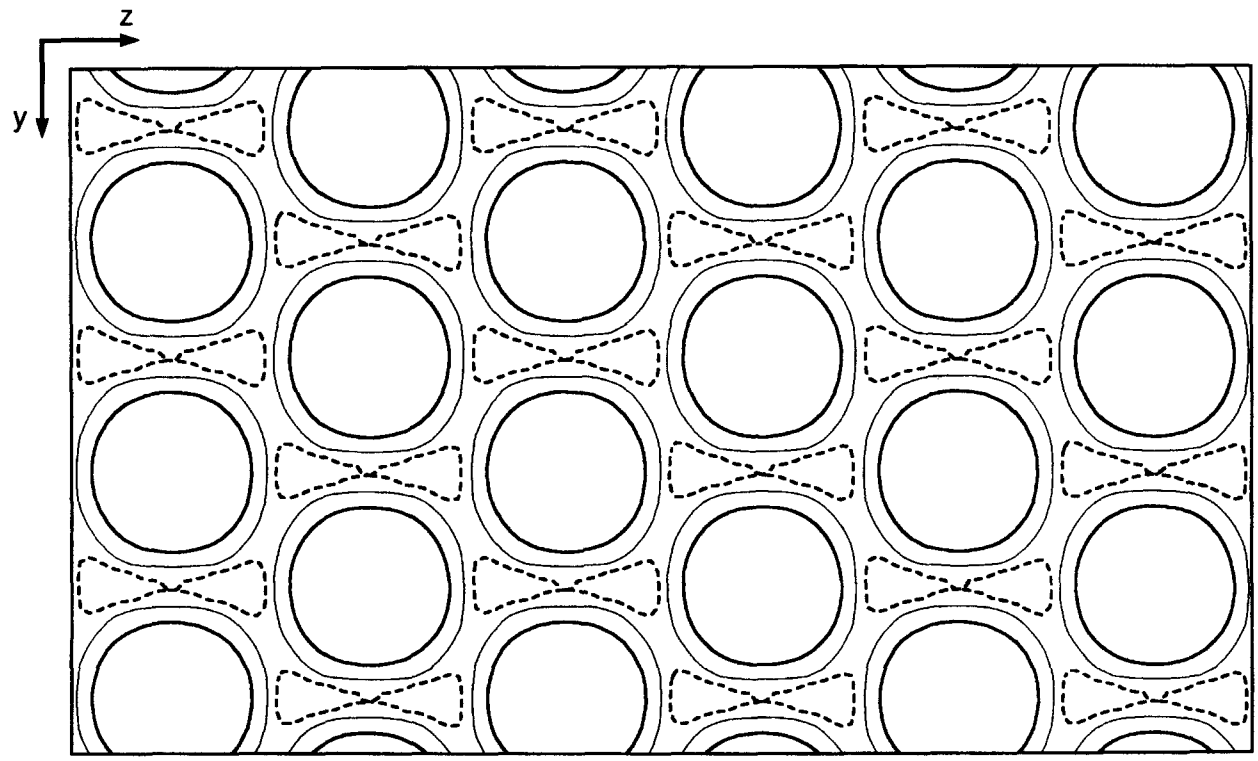

Figure 7 Distribution of the hexagonal cells for Le=1.0, λ_y=0.494, λ_z=0.855, A_0=0.056 (t=50); schematic domain is $3\lambda_y \times 3\lambda_z$; the amplitude is 0.160; solid, hair, and broken lines denote contours of the flame front at x=0.432, 0.512, 0.608, respectively

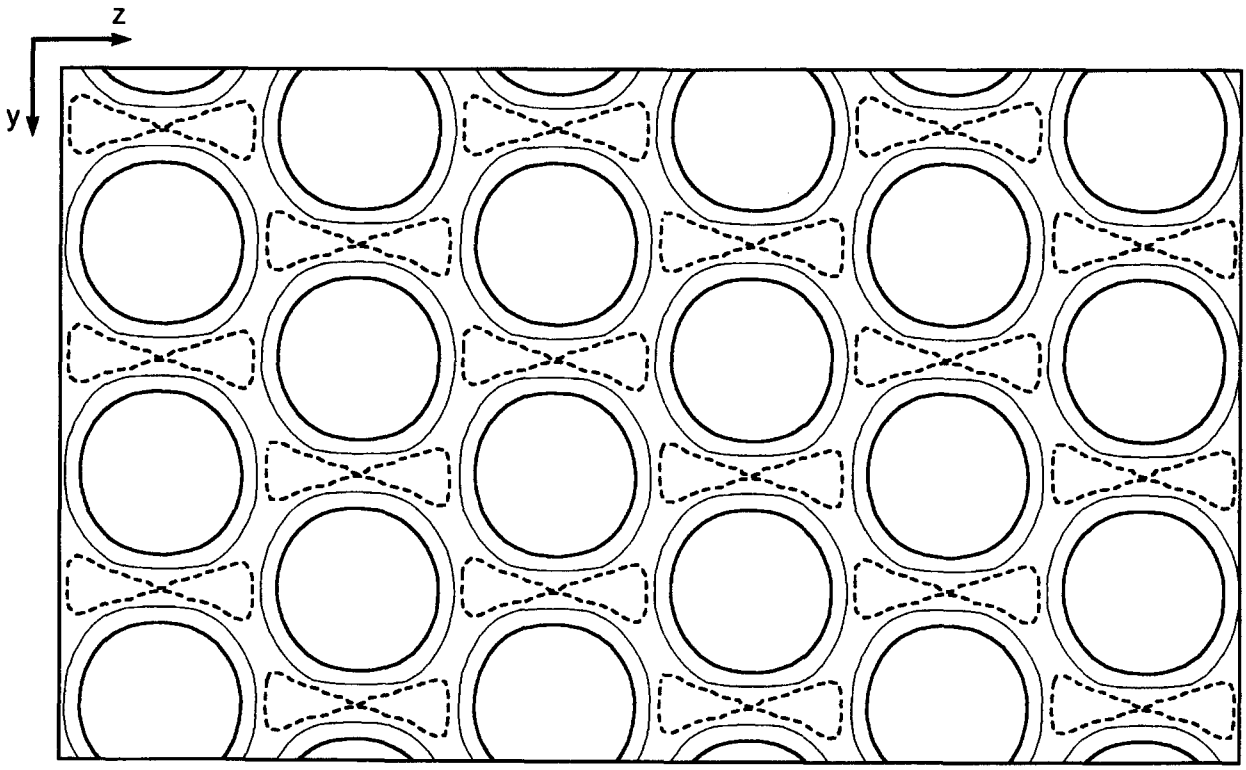

Figure 8 Distribution of the hexagonal cells for Le=1.2, $\lambda_y=0.666$, $\lambda_z=1.152$, $A_0=0.056$ ($t=90$); schematic domain is $3\lambda_y \times 3\lambda_z$; the amplitude is 0.180; solid, hair, and broken lines denote contours of the flame front at $x=0.423$, 0.513, 0.612, respectively

Finally, we research the mechanism of determination of the spacing between cells. There are disturbances with any wavelengths and with any amplitudes in the nature. Not all disturbance appear in the phenomena, but only elite disturbance evolves, and then the cellular flames are formed. On the plane flame, we superimpose the disturbance given by

$$\Sigma A_{0i} \sin(2\pi y/\lambda_{yi})\sin(2\pi z/\lambda_{zi}) \tag{8}$$

where

$$\lambda_{yi} = \lambda_{y\,\max}/i$$

$$(i = 1,2,\ldots,N)$$

$$\lambda_{zi} = \lambda_{z\,\max}/i$$

The structures of the flame fronts at $t=0$, 10 for Le = 0.5, $\lambda_{y\,\max}=0.498$, $\lambda_{z\,\max}=0.863$, $|A_{0i}|=1\times10^{-3}$, $N=8$ are illustrated in Figure 9. At $t=0$, there are the disturbances with some wavelengths on the flame. At $t=10$, the disturbance only with $\lambda_y=0.166$, $\lambda_z=0.288$ ($=\sqrt{3}\lambda_y$) is evolved. The distribution of the cells at $t=10$ is illustrated in Figure 10. It denotes that the wavelength of the elite disturbance is identical with the peculiar wavelength. Thus, we obtain the following relation on λ_3.

$$\lambda_3 = \frac{2}{\sqrt{3}}\frac{2\pi}{k_p} \tag{9}$$

In the 2-D flames, the cell size is written as

$$\lambda_2 = 2\pi/k_p \tag{10}$$

Therefore, the spacing between hexagonal cells of the 3-D flames is $2/\sqrt{3}$ times as long as the cell size of the 2-D flames. This relation is valid for other Lewis numbers and is in qualitative agreement with the experiment (Strehlow 1968).

Concluding remarks

We have investigated the flame instability based on the compressible Navier–Stokes equations. We have calculated the evolution of the disturbed flame to examine the hydrodynamic and diffusive-thermal effects and to study the mechanism of the cellular flame formation. The results are summarized as follows.

(1) We show numerically that the disturbances with sufficiently small amplitudes grow exponentially with time, as predicted in the linear analysis, and obtain the growth rates depending on the absolute values of the wave-number vectors. The dispersion relation in the 3-D field is consistent with that in the 2-D field. Thus, we can similarly treat both fields on the instability of premixed plane flames.

(2) The hydrodynamic effect has a destabilizing influence, and the growth rates are positive for small wave numbers. However, there is the marginal wave number, because the finite preheat zone thickness is taken into account. The flames are stable/unstable for disturbances with wave numbers larger/smaller than the marginal wave number. Thus, the flames shorter/longer than the marginal wavelength are stable/unstable. The diffusive-thermal effect has a great influence on the flame instability. The growth rates in-

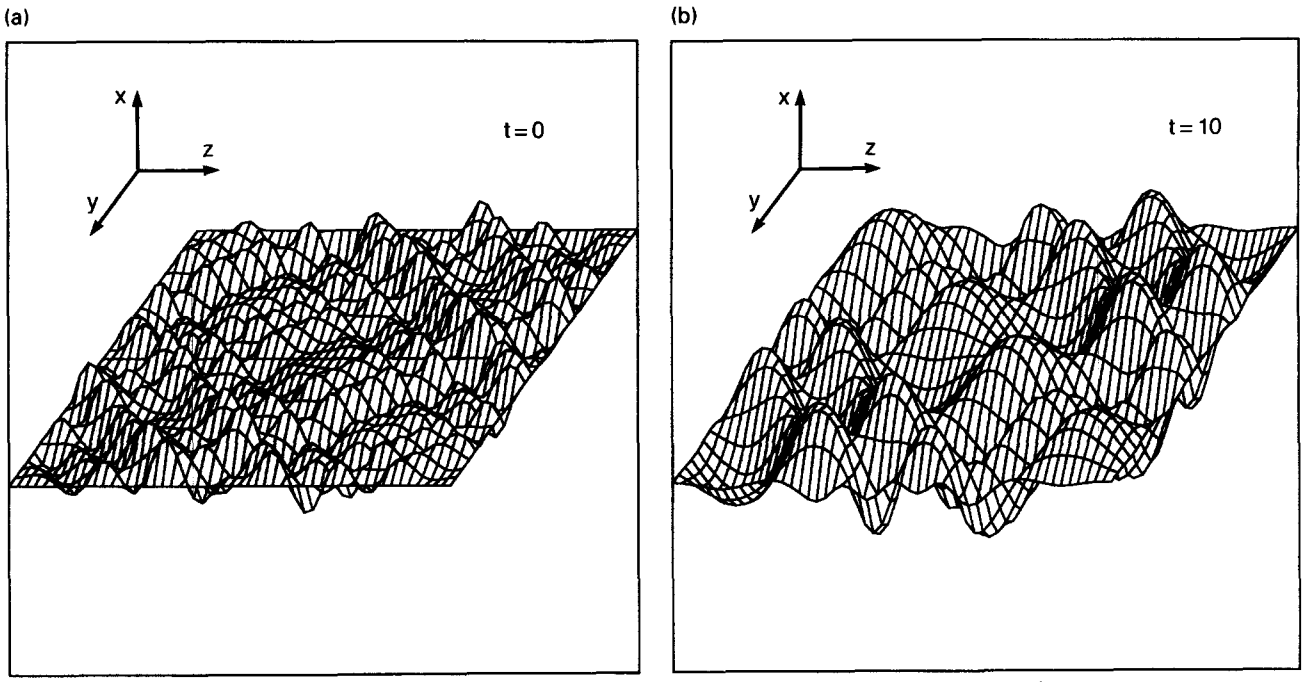

Figure 9 Structures of the flame fronts for Le=0.5, $\lambda_{ymax}=0.498$, $\lambda_{zmax}=0.863$, $A_0=3.8\times10^{-3}$ ($t=0, 10$)

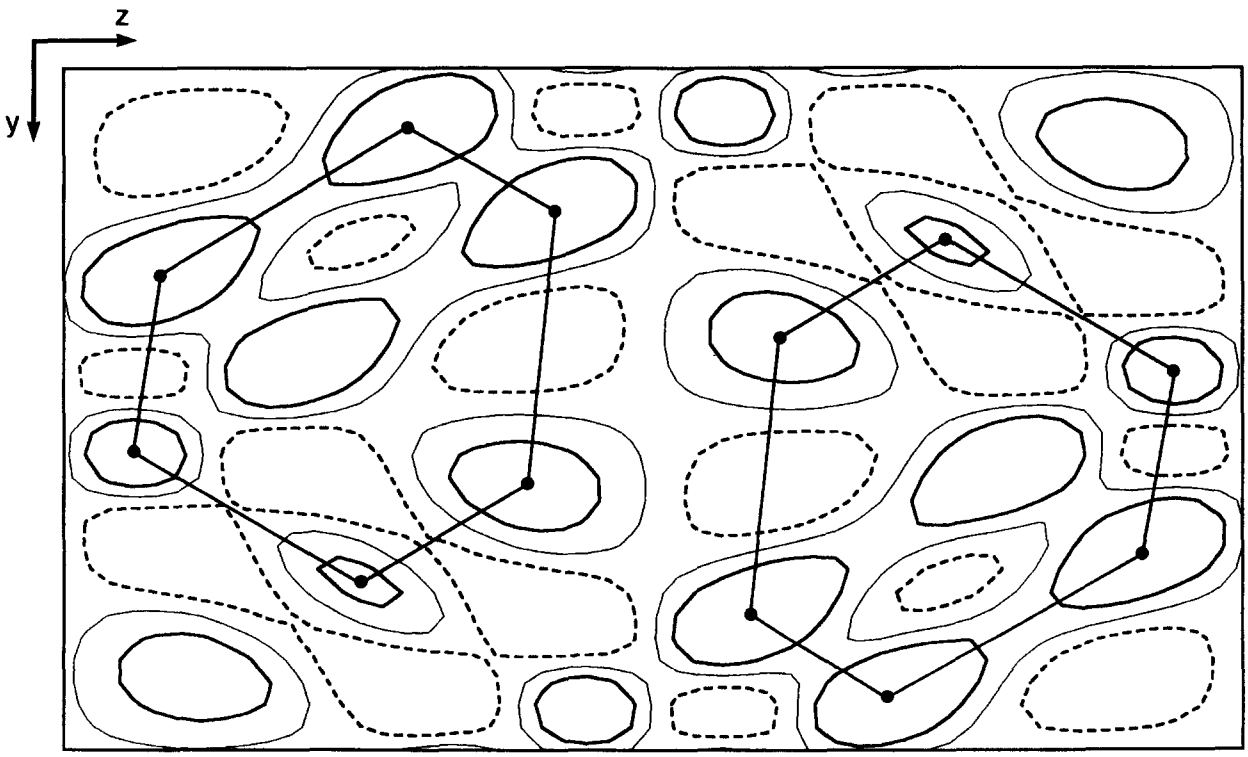

Figure 10 Distribution of the cells for Le=0.5, $\lambda_{ymax}=0.498$, $\lambda_{zmax}=0.863$, $A_0=3.8\times10^{-3}$ ($t=10$); solid, hair, and broken lines denote contours of the flame front at $x=0.4923$, 0.4945, 0.4967, respectively

crease/decrease, and the unstable region becomes wider/narrower for $Le < 1/Le > 1$, because the diffusive-thermal effect has a destabilizing/stabilizing influence for $Le < 1/Le > 1$.

(3) We produce the hexagonal cellular structure of the flame front not only for $Le < 1$ but also for $Le > 1$. The spacing between cells in flames for $Le < 1$ is small compared to that for $Le > 1$. Moreover, we show that the spacing of the 3-D flames is $2/\sqrt{3}$ times as long as the cell size of the 2-D flames.

References

Barenblatt, G. I., Zeldovich, Y. B. and Istratov, A. G. 1962. On diffusive-thermal stability of a laminar flame. *J. Appl. Mech. Tech. Phys.*, **4**, 21–26

Bregeon, B., Gordon, A. S. and Williams, F. A. 1978. Near-limit downward propagation of hydrogen and methane flames in oxygen-nitrogen mixtures. *Combust. Flame*, **33**, 33–45

Christopherson, D. G. 1940. Note on the vibration of membranes. *Quarterly J. Math.*, **11**, 63–65

Darrieus, G. 1938. Unpublished works presented at La Technique Moderne

Denet, B. 1993. On non-linear instabilities of cellular premixed flames. *Combust. Sci. Technol.*, **92**, 123–144

Denet, B. and Haldenwang, P. 1992. Numerical study of thermal-diffusive instability of premixed flames. *Combust. Sci. Technol.* **86**, 199–221

Denet, B. and Haldenwang, P. 1995. A numerical study of premixed flames Darrieus-Landau instability. *Combust. Sci. Technol.*, **104**, 143–167

Frankel, M. L. and Sivashinsky, G. I. 1982. The effect of viscosity on hydrodynamic stability of a plane flame front. *Combust. Sci. Technol.*, **29**, 207–224

Joulin, G. and Mitani, T. 1981. Linear stability analysis of two-reactant flames. *Combust. Flame*, **40**, 235–246

Kadowaki, S. 1994. Hydrodynamic flame instability and cellular flame formation. *Nensho no Kagaku to Gijutsu* (Japanese language companion publication to *Combust. Sci. Technol.*), **2**, 193–200

Kadowaki, S. 1995a. Instability of a deflagration wave propagating with finite Mach number. *Phys. Fluids*, **7**, 220–222

Kadowaki, S. 1995b. Numerical analysis on instability of cylindrical flames. *Combust. Sci. Technol.*, **107**, 181–193

Kadowaki, S. and Tsuge, S. 1985. On the critical stability of a plane flame with a preheat zone of finite thickness. *Trans. Japan Soc. Aero. Space Sci.* **28**, 108–119

Landau, L. D. 1944. On the theory of slow combustion. *Acta Phys.*, **19**, 77–85

Law, C. K. 1988. Dynamics of stretched flames. *Proc. 22nd Int. Symposium on Combustion*, The Combustion Institute, Pittsburgh, PA, 1381–1402

Markstein, G. H. 1951. Experimental and theoretical studies of flame-front stability. *J. Aeronaut. Sci.*, **18**, 199–209

Matalon, M. and Matkowsky, B. J. 1982. Flames as gasdynamic discontinuities. *J. Fluid Mech.*, **124**, 239–259

Michelson, D. M. and Sivashinsky, G. I. 1982. Thermal-expansion induced cellular flames. *Combust. Flame*, **48**, 211–217

Mitani, T. and Williams, F. A. 1980. Studies of cellular flames in hydrogen-oxygen-nitrogen mixtures. *Combust. Flame*, **39**, 169–190

Patnaik, G., Kailasanath, K., Oran, E. S. and Laskey, K. J. 1988. Detailed numerical simulations of cellular flames. *Proc. 22nd Int. Symposium on Combustion*, The Combustion Institute, Pittsburgh, PA, 1517–1526

Pelce, P. and Clavin, P. 1982. Influence of hydrodynamics and diffusion upon the stability limits of laminar premixed flames. *J. Fluid Mech.*, **124**, 219–237

Searby, G. and Quinard, J. 1990. Direct and indirect measurements of Markstein numbers of premixed flames. *Combust. Flame*, **82**, 298–311

Sivashinsky, G. I. 1977. Diffusion-thermal theory of cellular flames. *Combust. Sci. Technol.*, **15**, 137–146

Strehlow, R. A. 1968. *Fundamentals of Combustion*. International Textbook Company, Scranton, PA, chap. 7

Thual, O., Frisch, U. and Henon, M. 1985. Application of pole decomposition to an equation governing the dynamics of wrinkled flame fronts. *J. Physique*, **46**, 1485–1494

Williams, F. A. 1985. Combustion Theory, 2nd ed. Benjamin/Cummings, Menlo Park, CA, chap. 9